

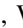





Publication Year	2019
Acceptance in OA @INAF	2023-05-24T14:28:10Z
Title	A Fermi Gamma-Ray Burst Monitor Search for Electromagnetic Signals Coincident with Gravitational-wave Candidates in Advanced LIGO's First Observing Run
Authors	Burns, E.; Goldstein, A.; Hui, C. M.; Blackburn, L.; Briggs, M. S.; et al.
DOI	10.3847/1538-4357/aaf726
Handle	http://hdl.handle.net/20.500.12386/34192
Journal	THE ASTROPHYSICAL JOURNAL
Number	871

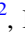







A *Fermi* Gamma-Ray Burst Monitor Search for Electromagnetic Signals Coincident with Gravitational-wave Candidates in Advanced LIGO's First Observing Run

E. Burns¹, A. Goldstein², C. M. Hui³, L. Blackburn^{4,5} , M. S. Briggs^{6,7}, V. Connaughton², R. Hamburg^{6,7}, D. Kocevski³, P. Veres⁷ , C. A. Wilson-Hodge³, E. Bissaldi^{8,9} , W. H. Cleveland², M. M. Giles¹⁰, B. Mailyan⁷, C. A. Meegan⁷, W. A. Paciesas², S. Poolakkil^{6,7}, R. D. Preece⁶, J. L. Racusin¹, O. J. Roberts², A. von Kienlin¹¹ 

(*Fermi* Gamma-Ray Burst Monitor),

and

B. P. Abbott¹², R. Abbott¹², T. D. Abbott¹³, F. Acernese^{14,15}, K. Ackley¹⁶, C. Adams¹⁷, T. Adams¹⁸, P. Addresso¹⁹, R. X. Adhikari¹², V. B. Adya^{20,21}, C. Affeldt^{20,21}, B. Agarwal²², M. Agathos²³, K. Agatsuma²⁴, N. Aggarwal⁵, O. D. Aguirre²⁵, L. Aiello^{26,27}, A. Ain²⁸, P. Ajith²⁹, B. Allen^{20,21,30}, G. Allen²², A. Allocca^{31,32}, M. A. Aloy³³, P. A. Altin³⁴, A. Amato³⁵, A. Ananyeva¹², S. B. Anderson¹², W. G. Anderson³⁰, S. V. Angelova³⁶, S. Antier³⁷, S. Appert¹², K. Arai¹², M. C. Araya¹², J. S. Areeda³⁸, M. Arène³⁹, N. Arnaud^{37,40}, K. G. Arun⁴¹, S. Ascenzi^{42,43}, G. Ashton¹⁶, M. Ast⁴⁴, S. M. Aston¹⁷, P. Astone⁴⁵, D. V. Atallah⁴⁶, F. Aubin¹⁸, P. Aufmuth²¹, C. Aulbert²⁰ , K. AultONeal⁴⁷, C. Austin¹³, A. Avila-Alvarez³⁸, S. Babak^{39,48}, P. Bacon³⁹, F. Badaracco^{26,27}, M. K. M. Bader²⁴, S. Bae⁴⁹, P. T. Baker⁵⁰, F. Baldaccini^{51,52}, G. Ballardin⁴⁰, S. W. Ballmer⁵³, S. Banagiri⁵⁴, J. C. Barayoga¹², S. E. Barclay⁵⁵, B. C. Barish¹², D. Barker⁵⁶, K. Barkett⁵⁷, S. Barnum⁵, F. Barone^{14,15}, B. Barr⁵⁵, L. Barsotti⁵, M. Barsuglia³⁹, D. Barta⁵⁸, J. Bartlett⁵⁶, I. Bartos⁵⁹ , R. Bassiri⁶⁰, A. Basti^{31,32}, J. C. Batch⁵⁶, M. Bawaj^{52,61}, J. C. Bayley⁵⁵, M. Bazzan^{62,63}, B. Bécsy⁶⁴ , C. Beer²⁰ , M. Bejger⁶⁵ , I. Belahcene³⁷, A. S. Bell⁵⁵, D. Beniwal⁶⁶, M. Bensch^{20,21}, B. K. Berger¹², G. Bergmann^{20,21}, S. Bernuzzi^{67,68} , J. J. Bero⁶⁹, C. P. L. Berry⁷⁰, D. Bersanetti⁷¹, A. Bertolini²⁴, J. Betzwieser¹⁷, R. Bhandare⁷², I. A. Bilenko⁷³, S. A. Bilgili⁵⁰, G. Billingsley¹², C. R. Billman⁵⁹, J. Birch¹⁷, R. Birney³⁶, O. Birnholtz⁶⁹, S. Biscans^{5,12}, S. Biscoveanu¹⁶, A. Bisht^{20,21}, M. Bitossi^{32,40}, M. A. Bizouard³⁷, J. K. Blackburn¹², J. Blackman⁵⁷, C. D. Blair¹⁷, D. G. Blair⁷⁴, R. M. Blair⁵⁶, S. Bloemen⁷⁵, O. Bock²⁰, N. Bode^{20,21}, M. Boer⁷⁶, Y. Boetzel⁷⁷, G. Bogaert⁷⁶, A. Bohe⁴⁸, F. Bondu⁷⁸, E. Bonilla⁶⁰, R. Bonnand¹⁸, P. Booker^{20,21}, B. A. Boom²⁴, C. D. Booth⁴⁶, R. Bork¹², V. Boschi⁴⁰, S. Bose^{28,79}, K. Bossie¹⁷, V. Bossilkov⁷⁴, J. Bosveld⁷⁴, Y. Bouffanais³⁹, A. Bozzi⁴⁰, C. Bradaschia³², P. R. Brady³⁰, A. Bramley¹⁷, M. Branchesi^{26,27}, J. E. Brau⁸⁰, T. Briant⁸¹, F. Brighenti^{82,83}, A. Brillet⁷⁶, M. Brinkmann^{20,21}, V. Brisson^{37,178}, P. Brockill³⁰, A. F. Brooks¹², D. D. Brown⁶⁶, S. Brunett¹², C. C. Buchanan¹³, A. Buikema⁵, T. Bulik⁸⁴, H. J. Bulten^{24,85}, A. Buonanno^{48,86}, D. Buskulic¹⁸, C. Buy³⁹, R. L. Byer⁶⁰, M. Cabero²⁰, L. Cadonati⁸⁷, G. Cagnoli^{35,88}, C. Cahillane¹², J. Calderón Bustillo⁸⁷, T. A. Callister¹², E. Calloni^{15,89}, J. B. Camp¹, M. Canepa^{71,90}, P. Canizares⁷⁵, K. C. Cannon⁹¹, H. Cao⁶⁶, J. Cao⁹², C. D. Capano²⁰, E. Capocasa³⁹, F. Carbognani⁴⁰, S. Caride⁹³, M. F. Carney⁹⁴, J. Casanueva Diaz³², C. Casentini^{42,43}, S. Caudill^{24,30}, M. Cavaglia⁹⁵, F. Cavalier³⁷, R. Cavallieri⁴⁰, G. Cella³², C. B. Cepeda¹², P. Cerdá-Durán³³, G. Cerretani^{31,32}, E. Cesarini^{43,96}, O. Chaibi⁷⁶, S. J. Chamberlin⁹⁷, M. Chan⁵⁵, S. Chao⁹⁸, P. Charlton⁹⁹, E. Chase¹⁰⁰, E. Chassande-Mottin³⁹, D. Chatterjee³⁰, B. D. Cheeseboro⁵⁰, H. Y. Chen¹⁰¹, X. Chen⁷⁴, Y. Chen⁵⁷, H.-P. Cheng⁵⁹, H. Y. Chia⁵⁹, A. Chincarini⁷¹, A. Chiummo⁴⁰, T. Chmiel⁹⁴, H. S. Cho¹⁰², M. Cho⁸⁶, J. H. Chow³⁴, N. Christensen^{76,103}, Q. Chu⁷⁴, A. J. K. Chua⁵⁷, S. Chua⁸¹, K. W. Chung¹⁰⁴, S. Chung⁷⁴, G. Ciani^{59,62,63}, A. A. Ciobanu⁶⁶, R. Ciolfi^{105,106} , F. Cipriano⁷⁶, C. E. Cirelli⁶⁰, A. Cirone^{71,90}, F. Clara⁵⁶, J. A. Clark⁸⁷, P. Clearwater¹⁰⁷, F. Cleva⁷⁶, C. Cocchieri⁹⁵, E. Coccia^{26,27}, P.-F. Cohadon⁸¹, D. Cohen³⁷, A. Colla^{45,108}, C. G. Collette¹⁰⁹, C. Collins⁷⁰, L. R. Cominsky¹¹⁰, M. Constancio Jr.²⁵, L. Conti⁶³, S. J. Cooper⁷⁰, P. Corban¹⁷, T. R. Corbitt¹³, I. Cordero-Carrión¹¹¹, K. R. Corley¹¹², N. Cornish¹¹³ , A. Corsi⁹³ , S. Cortese⁴⁰, C. A. Costa²⁵, R. Cotesta⁴⁸, M. W. Coughlin¹² , S. B. Coughlin^{46,100}, J.-P. Coulon⁷⁶, S. T. Countryman¹¹², P. Couvares¹², P. B. Covas¹¹⁴, E. E. Cowan⁸⁷, D. M. Coward⁷⁴, M. J. Cowart¹⁷, D. C. Coyne¹², R. Coyne¹¹⁵, J. D. E. Creighton³⁰, T. D. Creighton¹¹⁶, J. Cripe¹³, S. G. Crowder¹¹⁷, T. J. Cullen¹³, A. Cumming⁵⁵, L. Cunningham⁵⁵, E. Cuoco⁴⁰, T. Dal Canton¹, G. Dálya⁶⁴, S. L. Danilishin^{20,21}, S. D'Antonio⁴³, K. Danzmann^{20,21}, A. Dasgupta¹¹⁸, C. F. Da Silva Costa⁵⁹, V. Dattilo⁴⁰, I. Dave⁷², M. Davies³⁷, D. Davis⁵³, E. J. Daw¹¹⁹, B. Day⁸⁷, D. DeBra⁶⁰, M. Deenadayalan²⁸, J. Degallaix³⁵, M. De Laurentis^{15,89}, S. Deléglise⁸¹, W. Del Pozzo^{31,32}, N. Demos⁵, T. Denker^{20,21}, T. Dent²⁰, R. De Pietri^{67,68}, J. Derby³⁸, V. Dergachev²⁰, R. De Rosa^{15,89}, C. De Rossi^{35,40}, R. DeSalvo¹²⁰, O. de Varona^{20,21}, S. Dhurandhar²⁸, M. C. Díaz¹¹⁶, L. Di Fiore¹⁵, M. Di Giovanni^{106,121}, T. Di Girolamo^{15,89}, A. Di Lieto^{31,32}, B. Ding¹⁰⁹, S. Di Pace^{45,108}, I. Di Palma^{45,108}, F. Di Renzo^{31,32}, A. Dmitriev⁷⁰, Z. Doctor¹⁰¹ , V. Dolique³⁵, F. Donovan⁵, K. L. Dooley^{46,95}, S. Doravari^{20,21}, I. Dorrington⁴⁶, M. Dovale Álvarez⁷⁰, T. P. Downes³⁰, M. Drago^{20,26,27}, C. Dreissigacker^{20,21}, J. C. Driggers⁵⁶, Z. Du⁹², P. Dupej⁵⁵, S. E. Dwyer⁵⁶, P. J. Easter¹⁶, T. B. Edo¹¹⁹, M. C. Edwards¹⁰³, A. Effler¹⁷, H.-B. Eggenstein^{20,21} , P. Ehrens¹², J. Eichholz¹², S. S. Eikenberry⁵⁹, M. Eisenmann¹⁸, R. A. Eisenstein⁵, R. C. Essick¹⁰¹, H. Estelles¹¹⁴, D. Estevez¹⁸, Z. B. Etienne⁵⁰, T. Etzel¹², M. Evans⁵, T. M. Evans¹⁷, V. Fafone^{26,42,43}, H. Fair⁵³, S. Fairhurst⁴⁶ , X. Fan⁹², S. Farinon⁷¹, B. Farr⁸⁰ , W. M. Farr⁷⁰ , E. J. Fauchon-Jones⁴⁶, M. Favata¹²², M. Fays⁴⁶, C. Fee⁹⁴, H. Fehrmann²⁰, J. Feicht¹², M. M. Fejer⁶⁰, F. Feng³⁹, A. Fernandez-Galiana⁵, I. Ferrante^{31,32}, E. C. Ferreira²⁵, F. Ferrini⁴⁰, F. Fidecaro^{31,32}, I. Fiori⁴⁰, D. Fiorucci³⁹, M. Fishbach¹⁰¹ , R. P. Fisher⁵³, J. M. Fishner⁵, M. Fitz-Axen⁵⁴, R. Flaminio^{18,123}, M. Fletcher⁵⁵, H. Fong¹²⁴, J. A. Font^{33,125}, P. W. F. Forsyth³⁴, S. S. Forsyth⁸⁷, J.-D. Fournier⁷⁶, S. Frasca^{45,108}, F. Frasconi³², Z. Frei⁶⁴, A. Freise⁷⁰, R. Frey⁸⁰, V. Frey³⁷, P. Fritschel⁵, V. V. Frolov¹⁷, P. Fulda⁵⁹, M. Fyffe¹⁷, H. A. Gabbard⁵⁵, B. U. Gadre²⁸, S. M. Gaebel⁷⁰, J. R. Gair¹²⁶, L. Gammaitoni⁵¹, M. R. Ganija⁶⁶, S. G. Gaonkar²⁸, A. Garcia³⁸, C. García-Quirós¹¹⁴, F. Garufi^{15,89}, B. Gateley⁵⁶, S. Gaudio⁴⁷,

G. Gaur¹²⁷, V. Gayathri¹²⁸, G. Gemme⁷¹, E. Genin⁴⁰, A. Gennai³², D. George²², J. George⁷², L. Gergely¹²⁹, V. Germain¹⁸, S. Ghonge⁸⁷, Abhirup Ghosh²⁹, Archisman Ghosh²⁴, S. Ghosh³⁰, B. Giacomazzo^{106,121}, J. A. Giaime^{13,17}, K. D. Giardino¹⁷, A. Giazotto^{32,179}, K. Gill⁴⁷, G. Giordano^{14,15}, L. Glover¹²⁰, E. Goetz⁵⁶, R. Goetz⁵⁹, B. Goncharov¹⁶, G. González¹³, J. M. Gonzalez Castro^{31,32}, A. Gopakumar¹³⁰, M. L. Gorodetsky⁷³, S. E. Gossan¹², M. Gosselin⁴⁰, R. Gouaty¹⁸, A. Grado^{15,131}, C. Graef⁵⁵, M. Granata³⁵, A. Grant⁵⁵, S. Gras⁵, C. Gray⁵⁶, G. Greco^{82,83}, A. C. Green⁷⁰, R. Green⁴⁶, E. M. Gretarsson⁴⁷, P. Groot⁷⁵, H. Grote⁴⁶, S. Grunewald⁴⁸, P. Gruning³⁷, G. M. Guidi^{82,83}, H. K. Gulati¹¹⁸, X. Guo⁹², A. Gupta⁹⁷, M. K. Gupta¹¹⁸, K. E. Gushwa¹², E. K. Gustafson¹², R. Gustafson¹³², O. Halim^{26,27}, B. R. Hall⁷⁹, E. D. Hall⁵, E. Z. Hamilton⁴⁶, H. F. Hamilton¹³³, G. Hammond⁵⁵, M. Haney⁷⁷, M. M. Hanke^{20,21}, J. Hanks⁵⁶, C. Hanna⁹⁷, M. D. Hannam⁴⁶, O. A. Hannuksela¹⁰⁴, J. Hanson¹⁷, T. Hardwick¹³, J. Harms^{26,27}, G. M. Harry¹³⁴, I. W. Harry⁴⁸, M. J. Hart⁵⁵, C.-J. Haster¹²⁴, K. Haughian⁵⁵, J. Healy⁶⁹, A. Heidmann⁸¹, M. C. Heintze¹⁷, H. Heitmann⁷⁶, P. Hello³⁷, G. Hemming⁴⁰, M. Hendry⁵⁵, I. S. Heng⁵⁵, J. Hennig⁵⁵, A. W. Heptonstall¹², F. J. Hernandez¹⁶, M. Heurs^{20,21}, S. Hild⁵⁵, T. Hinderer⁷⁵, D. Hoak⁴⁰, S. Hochheim^{20,21}, D. Hofman³⁵, N. A. Holland³⁴, K. Holt¹⁷, D. E. Holz¹⁰¹, P. Hopkins⁴⁶, C. Horst³⁰, J. Hough⁵⁵, E. A. Houston⁵⁵, E. J. Howell⁷⁴, A. Hreibi⁷⁶, E. A. Huerta²², D. Huet³⁷, B. Hughey⁴⁷, M. Hulko¹², S. Husa¹¹⁴, S. H. Huttner⁵⁵, T. Huynh-Dinh¹⁷, A. Iess^{42,43}, N. Indik²⁰, C. Ingram⁶⁶, R. Inta⁹³, G. Intini^{45,108}, H. N. Isa⁵⁵, J.-M. Isac⁸¹, M. Isi¹², B. R. Iyer²⁹, K. Izumi⁵⁶, T. Jacqmin⁸¹, K. Jani⁸⁷, P. Jaranowski¹³⁵, D. S. Johnson²², W. W. Johnson¹³, D. I. Jones¹³⁶, R. Jones⁵⁵, R. J. G. Jonker²⁴, L. Ju⁷⁴, J. Junker^{20,21}, C. V. Kalaghatgi⁴⁶, V. Kalogera¹⁰⁰, B. Kamai¹², S. Kandhasamy¹⁷, G. Kang⁴⁹, J. B. Kanner¹², S. J. Kapadia³⁰, S. Karki⁸⁰, K. S. Karvinen^{20,21}, M. Kasprzak¹³, M. Katolik²², S. Katsanevas⁴⁰, E. Katsavounidis⁵, W. Katzman¹⁷, S. Kaufer^{20,21}, K. Kawabe⁵⁶, N. V. Keerthana²⁸, F. Kéfélian⁷⁶, D. Keitel⁵⁵, A. J. Kembal²², R. Kennedy¹¹⁹, J. S. Key¹³⁷, F. Y. Khalili⁷³, B. Khamesra⁸⁷, H. Khan³⁸, I. Khan^{26,43}, S. Khan²⁰, Z. Khan¹¹⁸, E. A. Khazanov¹³⁸, N. Kijbunchoo³⁴, Chunglee Kim¹³⁹, J. C. Kim¹⁴⁰, K. Kim¹⁰⁴, W. Kim⁶⁶, W. S. Kim¹⁴¹, Y.-M. Kim¹⁴², E. J. King⁶⁶, P. J. King⁵⁶, M. Kinley-Hanlon¹³⁴, R. Kirchhoff^{20,21}, J. S. Kissel⁵⁶, L. Kleybolte⁴⁴, S. Klimenko⁵⁹, T. D. Knowles⁵⁰, P. Koch^{20,21}, S. M. Koehlenbeck^{20,21}, S. Koley²⁴, V. Kondrashov¹², A. Kontos⁵, M. Korobko⁴⁴, W. Z. Korth¹², I. Kowalska⁸⁴, D. B. Kozak¹², C. Krämer²⁰, V. Kringel^{20,21}, B. Krishnan²⁰, A. Królak^{143,144}, G. Kuehn^{20,21}, P. Kumar¹⁴⁵, R. Kumar¹¹⁸, S. Kumar²⁹, L. Kuo⁹⁸, A. Kutynia¹⁴³, S. Kwang³⁰, B. D. Lackey⁴⁸, K. H. Lai¹⁰⁴, M. Landry⁵⁶, R. N. Lang¹⁴⁶, J. Lange⁶⁹, B. Lantz⁶⁰, R. K. Lanza⁵, A. Lartaux-Vollard³⁷, P. D. Lasky¹⁶, M. Laxen¹⁷, A. Lazzarini¹², C. Lazzaro⁶³, P. Leaci^{45,108}, S. Leavey^{20,21}, C. H. Lee¹⁰², H. K. Lee¹⁴⁷, H. M. Lee¹³⁹, H. W. Lee¹⁴⁰, K. Lee⁵⁵, J. Lehmann^{20,21}, A. Lenon⁵⁰, M. Leonardi^{20,21,123}, N. Leroy³⁷, N. Letendre¹⁸, Y. Levin¹⁶, J. Li⁹², T. G. F. Li¹⁰⁴, X. Li⁵⁷, S. D. Linker¹²⁰, T. B. Littenberg¹⁴⁸, J. Liu⁷⁴, X. Liu³⁰, R. K. L. Lo¹⁰⁴, N. A. Lockerbie³⁶, L. T. London⁴⁶, A. Longo^{149,150}, M. Lorenzini^{26,27}, V. Lorientte¹⁵¹, M. Lormand¹⁷, G. Losurdo³², J. D. Lough^{20,21}, C. O. Lousto⁶⁹, G. Lovelace³⁸, H. Lück^{20,21}, D. Lumaca^{42,43}, A. P. Lundgren²⁰, R. Lynch⁵, Y. Ma⁵⁷, R. Macas⁴⁶, S. Macfoy³⁶, B. Machenschalk²⁰, M. MacInnis⁵, D. M. Macleod⁴⁶, I. Magaña Hernandez³⁰, F. Magaña-Sandoval⁵³, L. Magaña Zertuche⁹⁵, R. M. Magee⁹⁷, E. Majorana⁴⁵, I. Maksimovic¹⁵¹, N. Man⁷⁶, V. Mandic⁵⁴, V. Mangano⁵⁵, G. L. Mansell³⁴, M. Manske^{30,34}, M. Mantovani⁴⁰, F. Marchesoni^{52,61}, F. Marion¹⁸, S. Márka¹¹², Z. Márka¹¹², C. Markakis²², A. S. Markosyan⁶⁰, A. Markowitz¹², E. Maros¹², A. Marquina¹¹¹, F. Martelli^{82,83}, L. Martellini⁷⁶, I. W. Martin⁵⁵, R. M. Martin¹²², D. V. Martynov⁵, K. Mason⁵, E. Massera¹¹⁹, A. Masserot¹⁸, T. J. Massinger¹², M. Masso-Reid⁵⁵, S. Mastrogiovanni^{45,108}, A. Matas⁵⁴, F. Matichard^{5,12}, L. Matone¹¹², N. Mavalvala⁵, N. Mazumder⁷⁹, J. J. McCann⁷⁴, R. McCarthy⁵⁶, D. E. McClelland³⁴, S. McCormick¹⁷, L. McCuller⁵, S. C. McGuire¹⁵², J. McIver¹², D. J. McManus³⁴, T. McRae³⁴, S. T. McWilliams⁵⁰, D. Meacher⁹⁷, G. D. Meadors¹⁶, M. Mehmet^{20,21}, J. Meidam²⁴, E. Mejuto-Villa¹⁹, A. Melatos¹⁰⁷, G. Mendell⁵⁶, D. Mendoza-Gandara^{20,21}, R. A. Mercer³⁰, L. Mereni³⁵, E. L. Merilh⁵⁶, M. Merzougui⁷⁶, S. Meshkov¹², C. Messenger⁵⁵, C. Messick⁹⁷, R. Metzdrorff⁸¹, P. M. Meyers⁵⁴, H. Miao⁷⁰, C. Michel³⁵, H. Middleton¹⁰⁷, E. E. Mikhailov¹⁵³, L. Milano^{15,89}, A. L. Miller⁵⁹, A. Miller^{45,108}, B. B. Miller¹⁰⁰, J. Miller⁵, M. Millhouse¹¹³, J. Mills⁴⁶, M. C. Milovich-Goff¹²⁰, O. Minazzoli^{76,154}, Y. Minenkov⁴³, J. Ming^{20,21}, C. Mishra¹⁵⁵, S. Mitra²⁸, V. P. Mitrofanov⁷³, G. Mitselmakher⁵⁹, R. Mittleman⁵, D. Moffa⁹⁴, K. Mogushi⁹⁵, M. Mohan⁴⁰, S. R. P. Mohapatra⁵, M. Montani^{82,83}, C. J. Moore²³, D. Moraru⁵⁶, G. Moreno⁵⁶, S. Morisaki⁹¹, B. Mours¹⁸, C. M. Mow-Lowry⁷⁰, G. Mueller⁵⁹, A. W. Muir⁴⁶, Arunava Mukherjee^{20,21}, D. Mukherjee³⁰, S. Mukherjee¹¹⁶, N. Mukund²⁸, A. Mullavey¹⁷, J. Munch⁶⁶, E. A. Muñoz⁵³, M. Muratore⁴⁷, P. G. Murray⁵⁵, A. Nagar^{96,156,157}, K. Napier⁸⁷, I. Nardecchia^{42,43}, L. Naticchioni^{45,108}, R. K. Nayak¹⁵⁸, J. Neilson¹²⁰, G. Nelemans^{24,75}, T. J. N. Nelson¹⁷, M. Nery^{20,21}, A. Neunzert¹³², L. Nevin¹², J. M. Newport¹³⁴, K. Y. Ng⁵, S. Ng⁶⁶, P. Nguyen⁸⁰, T. T. Nguyen³⁴, D. Nichols⁷⁵, A. B. Nielsen²⁰, S. Nissanke^{24,75}, A. Nitz²⁰, F. Nocera⁴⁰, D. Nolting¹⁷, C. North⁴⁶, L. K. Nuttall⁴⁶, M. Obergaulinger³³, J. Oberling⁵⁶, B. D. O'Brien⁵⁹, G. D. O'Dea¹²⁰, G. H. Ogil¹⁵⁹, J. J. Oh¹⁴¹, S. H. Oh¹⁴¹, F. Ohme²⁰, H. Ohta⁹¹, M. A. Okada²⁵, M. Oliver¹¹⁴, P. Oppermann^{20,21}, Richard J. Oram¹⁷, B. O'Reilly¹⁷, R. Ormiston⁵⁴, L. F. Ortega⁵⁹, R. O'Shaughnessy⁶⁹, S. Ossokine⁴⁸, D. J. Ottaway⁶⁶, H. Overmier¹⁷, B. J. Owen⁹³, A. E. Pace⁹⁷, G. Pagano^{31,32}, J. Page¹⁴⁸, M. A. Page⁷⁴, A. Pai¹²⁸, S. A. Pai⁷², J. R. Palamos⁸⁰, O. Palashov¹³⁸, C. Palomba⁴⁵, A. Pal-Singh⁴⁴, Howard Pan⁹⁸, Huang-Wei Pan⁹⁸, B. Pang⁵⁷, P. T. H. Pang¹⁰⁴, C. Pankow¹⁰⁰, F. Pannarale⁴⁶, B. C. Pant⁷², F. Paoletti³², A. Paoli⁴⁰, M. A. Papa^{20,21,30}, A. Parida²⁸, W. Parker¹⁷, D. Pascucci⁵⁵, A. Pasqualetti⁴⁰, R. Passaquieti^{31,32}, D. Passuello³², M. Patil¹⁴⁴, B. Patricelli^{32,160}, B. L. Pearlstone⁵⁵, C. Pedersen⁴⁶, M. Pedraza¹², R. Pedurand^{35,161}, L. Pekowsky⁵³, A. Pele¹⁷, S. Penn¹⁶², C. J. Perez⁵⁶, A. Perreca^{106,121}, L. M. Perri¹⁰⁰, H. P. Pfeiffer^{48,124}, M. Phelps⁵⁵, K. S. Phukon²⁸, O. J. Piccinni^{45,108}, M. Pichot⁷⁶, F. Piergiovanni^{82,83}, V. Pierro¹⁹, G. Pillant⁴⁰, L. Pinard³⁵, I. M. Pinto¹⁹, M. Pirello⁵⁶, M. Pitkin⁵⁵, R. Poggiani^{31,32}, P. Popolizio⁴⁰, E. K. Porter³⁹, L. Possenti^{83,163}, A. Post²⁰, J. Powell¹⁶⁴, J. Prasad²⁸, J. W. W. Pratt⁴⁷, G. Pratten¹¹⁴, V. Predoi⁴⁶, T. Prestegard³⁰, M. Principe¹⁹, S. Privitera⁴⁸, G. A. Prodi^{106,121}, L. G. Prokhorov⁷³, O. Puncken^{20,21}, M. Punturo⁵²,

P. Puppó⁴⁵, M. Pürer⁴⁸, H. Qi³⁰, V. Quetschke¹¹⁶, E. A. Quintero¹², R. Quitzow-James⁸⁰, F. J. Raab⁵⁶, D. S. Rabeling³⁴, H. Radkins⁵⁶, P. Raffai⁶⁴, S. Raja⁷², C. Rajan⁷², B. Rajbhandari⁹³, M. Rakhmanov¹¹⁶, K. E. Ramirez¹¹⁶, A. Ramos-Buades¹¹⁴, Javed Rana²⁸, P. Rapagnani^{45,108}, V. Raymond⁴⁶, M. Razzano^{31,32}, J. Read³⁸, T. Regimbau^{18,76}, L. Rei⁷¹, S. Reid³⁶, D. H. Reitze^{12,59}, W. Ren²², F. Ricci^{45,108}, P. M. Ricker²², K. Riles¹³², M. Rizzo⁶⁹, N. A. Robertson^{12,55}, R. Robie⁵⁵, F. Robinet³⁷, T. Robson¹¹³, A. Rocchi⁴³, L. Rolland¹⁸, J. G. Rollins¹², V. J. Roma⁸⁰, R. Romano^{14,15}, C. L. Romel⁵⁶, J. H. Romie¹⁷, D. Rosińska^{65,165}, M. P. Ross¹⁶⁶, S. Rowan⁵⁵, A. Rüdiger^{20,21}, P. Ruggi⁴⁰, G. Rutins¹⁶⁷, K. Ryan⁵⁶, S. Sachdev¹², T. Sadecki⁵⁶, M. Sakellariadou¹⁶⁸, L. Salconi⁴⁰, M. Saleem¹²⁸, F. Salemi²⁰, A. Samajdar^{24,158}, L. Sammut¹⁶, L. M. Sampson¹⁰⁰, E. J. Sanchez¹², L. E. Sanchez¹², N. Sanchis-Gual³³, V. Sandberg⁵⁶, J. R. Sanders⁵³, N. Sarin¹⁶, B. Sassolas³⁵, B. S. Sathyaprakash^{46,97}, P. R. Saulson⁵³, O. Sauter¹³², R. L. Savage⁵⁶, A. Sawadsky⁴⁴, P. Schale⁸⁰, M. Scheel⁵⁷, J. Scheuer¹⁰⁰, P. Schmidt⁷⁵, R. Schnabel⁴⁴, R. M. S. Schofield⁸⁰, A. Schönbeck⁴⁴, E. Schreiber^{20,21}, D. Schuette^{20,21}, B. W. Schulte^{20,21}, B. F. Schutz^{20,46}, S. G. Schwalbe⁴⁷, J. Scott⁵⁵, S. M. Scott³⁴, E. Seidel²², D. Sellers¹⁷, A. S. Sengupta¹⁶⁹, D. Sentenac⁴⁰, V. Sequino^{26,42,43}, A. Sergeev¹³⁸, Y. Setyawati²⁰, D. A. Shaddock³⁴, T. J. Shaffer⁵⁶, A. A. Shah¹⁴⁸, M. S. Shahriar¹⁰⁰, M. B. Shaner¹²⁰, L. Shao⁴⁸, B. Shapiro⁶⁰, P. Shawhan⁸⁶, H. Shen²², D. H. Shoemaker⁵, D. M. Shoemaker⁸⁷, K. Siellez⁸⁷, X. Siemens³⁰, M. Sieniawska⁶⁵, D. Sigg⁵⁶, A. D. Silva²⁵, L. P. Singer¹, A. Singh^{20,21}, A. Singhal^{26,45}, A. M. Sintes¹¹⁴, B. J. J. Slagmolen³⁴, T. J. Slaven-Blair⁷⁴, B. Smith¹⁷, J. R. Smith³⁸, R. J. E. Smith¹⁶, S. Somala¹⁷⁰, E. J. Son¹⁴¹, B. Sorazu⁵⁵, F. Sorrentino⁷¹, T. Souradeep²⁸, A. P. Spencer⁵⁵, A. K. Srivastava¹¹⁸, K. Staats⁴⁷, C. Stachie⁷⁶, M. Steinke^{20,21}, J. Steinlechner^{44,55}, S. Steinlechner⁴⁴, D. Steinmeyer^{20,21}, B. Steltner^{20,21}, S. P. Stevenson¹⁶⁴, D. Stocks⁶⁰, R. Stone¹¹⁶, D. J. Stops⁷⁰, K. A. Strain⁵⁵, G. Stratta^{82,83}, S. E. Strigin⁷³, A. Strunk⁵⁶, R. Sturani¹⁷¹, A. L. Stuver¹⁷², T. Z. Summerscales¹⁷³, L. Sun¹⁰⁷, S. Sunil¹¹⁸, J. Suresh²⁸, P. J. Sutton⁴⁶, B. L. Swinkels²⁴, M. J. Szczepańczyk⁴⁷, M. Tacca²⁴, S. C. Tait⁵⁵, C. Talbot¹⁶, D. Talukder⁸⁰, D. B. Tanner⁵⁹, M. Tápai¹²⁹, A. Taracchini⁴⁸, J. D. Tasson¹⁰³, J. A. Taylor¹⁴⁸, R. Taylor¹², S. V. Tewari¹⁶², T. Theeg^{20,21}, F. Thies^{20,21}, E. G. Thomas⁷⁰, M. Thomas¹⁷, P. Thomas⁵⁶, K. A. Thorne¹⁷, E. Thrane¹⁶, S. Tiwari^{26,106}, V. Tiwari⁴⁶, K. V. Tokmakov³⁶, K. Toland⁵⁵, M. Tonelli^{31,32}, Z. Tornasi⁵⁵, A. Torres-Forné³³, C. I. Torrie¹², D. Töyrä⁷⁰, F. Travasso^{40,52}, G. Traylor¹⁷, J. Trinastic⁵⁹, M. C. Tringali^{106,121}, L. Trozzo^{32,174}, K. W. Tsang²⁴, M. Tse⁵, R. Tso⁵⁷, D. Tsuna⁹¹, L. Tsukada⁹¹, D. Tuyenbayev¹¹⁶, K. Ueno³⁰, D. Ugolini¹⁷⁵, A. L. Urban¹², S. A. Usman⁴⁶, H. Vahlbruch^{20,21}, G. Vajente¹², G. Valdes¹³, N. van Bakel²⁴, M. van Beuzekom²⁴, J. F. J. van den Brand^{24,85}, C. Van Den Broeck^{24,176}, D. C. Vander-Hyde⁵³, L. van der Schaaf²⁴, J. V. van Heijningen²⁴, A. A. van Veggel⁵⁵, M. Vardaro^{62,63}, V. Varma⁵⁷, S. Vass¹², M. Vasúth⁵⁸, A. Vecchio⁷⁰, G. Vedovato⁶³, J. Veitch⁵⁵, P. J. Veitch⁶⁶, K. Venkateswara¹⁶⁶, G. Venugopalan¹², D. Verkindt¹⁸, F. Vetrano^{82,83}, A. Viceré^{82,83}, A. D. Viets³⁰, S. Vinciguerra⁷⁰, D. J. Vine¹⁶⁷, J.-Y. Vinet⁷⁶, S. Vitale⁵, T. Vo⁵³, H. Vocca^{51,52}, C. Vorvick⁵⁶, S. P. Vyatchanin⁷³, A. R. Wade¹², L. E. Wade⁹⁴, M. Wade⁹⁴, R. Walet²⁴, M. Walker³⁸, L. Wallace¹², S. Walsh^{20,30}, G. Wang^{26,32}, H. Wang⁷⁰, J. Z. Wang¹³², W. H. Wang¹¹⁶, Y. F. Wang¹⁰⁴, R. L. Ward³⁴, J. Warner⁵⁶, M. Was¹⁸, J. Watchi¹⁰⁹, B. Weaver⁵⁶, L.-W. Wei^{20,21}, M. Weinert^{20,21}, A. J. Weinstein¹², R. Weiss⁵, F. Wellmann^{20,21}, L. Wen⁷⁴, E. K. Wessel²², P. Weßels^{20,21}, J. Westerweck²⁰, K. Wette³⁴, J. T. Whelan⁶⁹, B. F. Whiting⁵⁹, C. Whittle⁵, D. Wilken^{20,21}, D. Williams⁵⁵, R. D. Williams¹², A. R. Williamson^{69,75}, J. L. Willis^{12,133}, B. Willke^{20,21}, M. H. Wimmer^{20,21}, W. Winkler^{20,21}, C. C. Wipf¹², H. Wittel^{20,21}, G. Woan⁵⁵, J. Woehler^{20,21}, J. K. Wofford⁶⁹, W. K. Wong¹⁰⁴, J. Worden⁵⁶, J. L. Wright⁵⁵, D. S. Wu^{20,21}, D. M. Wysocki⁶⁹, S. Xiao¹², W. Yam⁵, H. Yamamoto¹², C. C. Yancey⁸⁶, L. Yang¹⁷⁷, M. J. Yap³⁴, M. Yazback⁵⁹, Hang Yu⁵, Haocun Yu⁵, M. Yvert¹⁸, A. Zadrożny¹⁴³, M. Zanolin⁴⁷, T. Zelenova⁴⁰, J.-P. Zendri⁶³, M. Zevin¹⁰⁰, J. Zhang⁷⁴, L. Zhang¹², M. Zhang¹⁵³, T. Zhang⁵⁵, Y.-H. Zhang^{20,21}, C. Zhao⁷⁴, M. Zhou¹⁰⁰, Z. Zhou¹⁰⁰, S. J. Zhu^{20,21}, X. J. Zhu¹⁶, M. E. Zucker^{5,12}, and J. Zweizig¹²

(The LIGO Scientific Collaboration and the Virgo Collaboration)

- ¹ NASA Goddard Space Flight Center, Greenbelt, MD 20771, USA
- ² Science and Technology Institute, Universities Space Research Association, Huntsville, AL 35805, USA
- ³ NASA Marshall Space Flight Center, Huntsville, AL 35812, USA
- ⁴ Harvard-Smithsonian Center for Astrophysics, 60 Garden Street, Cambridge, MA 02138, USA
- ⁵ LIGO, Massachusetts Institute of Technology, Cambridge, MA 02139, USA
- ⁶ Department of Space Science, University of Alabama in Huntsville, Huntsville, AL 35899, USA
- ⁷ Center for Space Plasma and Aeronomic Research, University of Alabama in Huntsville, Huntsville, AL 35899, USA
- ⁸ Politecnico di Bari, Via Edoardo Orabona, 4, I-70126 Bari BA, Italy
- ⁹ Istituto Nazionale di Fisica Nucleare, Sezione di Bari, I-70126 Bari, Italy
- ¹⁰ Jacobs Space Exploration Group, Huntsville, AL 35806, USA
- ¹¹ Max-Planck-Institut für extraterrestrische Physik, Giessenbachstrasse 1, D-85748 Garching, Germany
- ¹² LIGO, California Institute of Technology, Pasadena, CA 91125, USA
- ¹³ Louisiana State University, Baton Rouge, LA 70803, USA
- ¹⁴ Università di Salerno, Fisciano, I-84084 Salerno, Italy
- ¹⁵ INFN, Sezione di Napoli, Complesso Universitario di Monte Sant'Angelo, I-80126 Napoli, Italy
- ¹⁶ OzGrav, School of Physics & Astronomy, Monash University, Clayton, VIC 3800, Australia
- ¹⁷ LIGO Livingston Observatory, Livingston, LA 70754, USA
- ¹⁸ Laboratoire d'Annecy de Physique des Particules (LAPP), Université Grenoble Alpes, Université Savoie Mont Blanc, CNRS/IN2P3, F-74941 Annecy, France
- ¹⁹ University of Sannio at Benevento, I-82100 Benevento, Italy and INFN, Sezione di Napoli, I-80100 Napoli, Italy
- ²⁰ Max Planck Institute for Gravitational Physics (Albert Einstein Institute), D-30167 Hannover, Germany
- ²¹ Leibniz Universität Hannover, D-30167 Hannover, Germany
- ²² NCSA, University of Illinois at Urbana-Champaign, Urbana, IL 61801, USA
- ²³ University of Cambridge, Cambridge CB2 1TN, UK
- ²⁴ Nikhef, Science Park 105, 1098 XG Amsterdam, The Netherlands
- ²⁵ Instituto Nacional de Pesquisas Espaciais, 12227-010 São José dos Campos, São Paulo, Brazil

- ²⁶ Gran Sasso Science Institute (GSSI), I-67100 L'Aquila, Italy
- ²⁷ INFN, Laboratori Nazionali del Gran Sasso, I-67100 Assergi, Italy
- ²⁸ Inter-University Centre for Astronomy and Astrophysics, Pune 411007, India
- ²⁹ International Centre for Theoretical Sciences, Tata Institute of Fundamental Research, Bengaluru 560089, India
- ³⁰ University of Wisconsin-Milwaukee, Milwaukee, WI 53201, USA
- ³¹ Università di Pisa, I-56127 Pisa, Italy
- ³² INFN, Sezione di Pisa, I-56127 Pisa, Italy
- ³³ Departamento de Astronomía y Astrofísica, Universitat de València, E-46100 Burjassot, València, Spain
- ³⁴ OzGrav, Australian National University, Canberra, ACT 0200, Australia
- ³⁵ Laboratoire des Matériaux Avancés (LMA), CNRS/IN2P3, F-69622 Villeurbanne, France
- ³⁶ SUPA, University of Strathclyde, Glasgow G1 1XQ, UK
- ³⁷ LAL, Université Paris-Sud, CNRS/IN2P3, Université Paris-Saclay, F-91898 Orsay, France
- ³⁸ California State University Fullerton, Fullerton, CA 92831, USA
- ³⁹ APC, AstroParticule et Cosmologie, Université Paris Diderot, CNRS/IN2P3, CEA/Irfu, Observatoire de Paris, Sorbonne Paris Cité, F-75205 Paris Cedex 13, France
- ⁴⁰ European Gravitational Observatory (EGO), I-56021 Cascina, Pisa, Italy
- ⁴¹ Chennai Mathematical Institute, Chennai 603103, India
- ⁴² Università di Roma Tor Vergata, I-00133 Roma, Italy
- ⁴³ INFN, Sezione di Roma Tor Vergata, I-00133 Roma, Italy
- ⁴⁴ Universität Hamburg, D-22761 Hamburg, Germany
- ⁴⁵ INFN, Sezione di Roma, I-00185 Roma, Italy
- ⁴⁶ Cardiff University, Cardiff CF24 3AA, UK
- ⁴⁷ Embry-Riddle Aeronautical University, Prescott, AZ 86301, USA
- ⁴⁸ Max Planck Institute for Gravitational Physics (Albert Einstein Institute), D-14476 Potsdam-Golm, Germany
- ⁴⁹ Korea Institute of Science and Technology Information, Daejeon 34141, Republic of Korea
- ⁵⁰ West Virginia University, Morgantown, WV 26506, USA
- ⁵¹ Università di Perugia, I-06123 Perugia, Italy
- ⁵² INFN, Sezione di Perugia, I-06123 Perugia, Italy
- ⁵³ Syracuse University, Syracuse, NY 13244, USA
- ⁵⁴ University of Minnesota, Minneapolis, MN 55455, USA
- ⁵⁵ SUPA, University of Glasgow, Glasgow G12 8QQ, UK
- ⁵⁶ LIGO Hanford Observatory, Richland, WA 99352, USA
- ⁵⁷ Caltech CaRT, Pasadena, CA 91125, USA
- ⁵⁸ Wigner RCP, RMKI, H-1121 Budapest, Konkoly Thege Miklós út 29-33, Hungary
- ⁵⁹ University of Florida, Gainesville, FL 32611, USA
- ⁶⁰ Stanford University, Stanford, CA 94305, USA
- ⁶¹ Università di Camerino, Dipartimento di Fisica, I-62032 Camerino, Italy
- ⁶² Università di Padova, Dipartimento di Fisica e Astronomia, I-35131 Padova, Italy
- ⁶³ INFN, Sezione di Padova, I-35131 Padova, Italy
- ⁶⁴ MTA-ELTE Astrophysics Research Group, Institute of Physics, Eötvös University, Budapest 1117, Hungary
- ⁶⁵ Nicolaus Copernicus Astronomical Center, Polish Academy of Sciences, 00-716, Warsaw, Poland
- ⁶⁶ OzGrav, University of Adelaide, Adelaide, SA 5005, Australia
- ⁶⁷ Dipartimento di Scienze Matematiche, Fisiche e Informatiche, Università di Parma, I-43124 Parma, Italy
- ⁶⁸ INFN, Sezione di Milano Bicocca, Gruppo Collegato di Parma, I-43124 Parma, Italy
- ⁶⁹ Rochester Institute of Technology, Rochester, NY 14623, USA
- ⁷⁰ University of Birmingham, Birmingham B15 2TT, UK
- ⁷¹ INFN, Sezione di Genova, I-16146 Genova, Italy
- ⁷² RRCAT, Indore, Madhya Pradesh 452013, India
- ⁷³ Faculty of Physics, Lomonosov Moscow State University, Moscow 119991, Russia
- ⁷⁴ OzGrav, University of Western Australia, Crawley, WA 6009, Australia
- ⁷⁵ Department of Astrophysics/IMAPP, Radboud University Nijmegen, P.O. Box 9010, 6500 GL Nijmegen, The Netherlands
- ⁷⁶ Artemis, Université Côte d'Azur, Observatoire Côte d'Azur, CNRS, CS 34229, F-06304 Nice Cedex 4, France
- ⁷⁷ Physik-Institut, University of Zurich, Winterthurerstrasse 190, 8057 Zurich, Switzerland
- ⁷⁸ Université de Rennes, CNRS, Institut FOTON—UMR6082, F-3500 Rennes, France
- ⁷⁹ Washington State University, Pullman, WA 99164, USA
- ⁸⁰ University of Oregon, Eugene, OR 97403, USA
- ⁸¹ Laboratoire Kastler Brossel, Sorbonne Université, CNRS, ENS-Université PSL, Collège de France, F-75005 Paris, France
- ⁸² Università degli Studi di Urbino 'Carlo Bo,' I-61029 Urbino, Italy
- ⁸³ INFN, Sezione di Firenze, I-50019 Sesto Fiorentino, Firenze, Italy
- ⁸⁴ Astronomical Observatory Warsaw University, 00-478 Warsaw, Poland
- ⁸⁵ VU University Amsterdam, 1081 HV Amsterdam, The Netherlands
- ⁸⁶ University of Maryland, College Park, MD 20742, USA
- ⁸⁷ School of Physics, Georgia Institute of Technology, Atlanta, GA 30332, USA
- ⁸⁸ Université Claude Bernard Lyon 1, F-69622 Villeurbanne, France
- ⁸⁹ Università di Napoli 'Federico II,' Complesso Universitario di Monte Sant'Angelo, I-80126 Napoli, Italy
- ⁹⁰ Dipartimento di Fisica, Università degli Studi di Genova, I-16146 Genova, Italy
- ⁹¹ RESCEU, University of Tokyo, Tokyo, 113-0033, Japan
- ⁹² Tsinghua University, Beijing 100084, People's Republic of China
- ⁹³ Texas Tech University, Lubbock, TX 79409, USA
- ⁹⁴ Kenyon College, Gambier, OH 43022, USA
- ⁹⁵ The University of Mississippi, Mississippi, MS 38677, USA
- ⁹⁶ Museo Storico della Fisica e Centro Studi e Ricerche "Enrico Fermi," I-00184 Roma, Italy
- ⁹⁷ The Pennsylvania State University, University Park, PA 16802, USA
- ⁹⁸ National Tsing Hua University, Hsinchu City, 30013 Taiwan, People's Republic of China
- ⁹⁹ Charles Sturt University, Wagga Wagga, NSW 2678, Australia

- ¹⁰⁰ Center for Interdisciplinary Exploration & Research in Astrophysics (CIERA), Northwestern University, Evanston, IL 60208, USA
- ¹⁰¹ University of Chicago, Chicago, IL 60637, USA
- ¹⁰² Pusan National University, Busan 46241, Republic of Korea
- ¹⁰³ Carleton College, Northfield, MN 55057, USA
- ¹⁰⁴ The Chinese University of Hong Kong, Shatin, NT, Hong Kong
- ¹⁰⁵ INAF, Osservatorio Astronomico di Padova, I-35122 Padova, Italy
- ¹⁰⁶ INFN, Trento Institute for Fundamental Physics and Applications, I-38123 Povo, Trento, Italy
- ¹⁰⁷ OzGrav, University of Melbourne, Parkville, VIC 3010, Australia
- ¹⁰⁸ Università di Roma 'La Sapienza,' I-00185 Roma, Italy
- ¹⁰⁹ Université Libre de Bruxelles, Brussels B-1050, Belgium
- ¹¹⁰ Sonoma State University, Rohnert Park, CA 94928, USA
- ¹¹¹ Departamento de Matemáticas, Universitat de València, E-46100 Burjassot, València, Spain
- ¹¹² Columbia University, New York, NY 10027, USA
- ¹¹³ Montana State University, Bozeman, MT 59717, USA
- ¹¹⁴ Universitat de les Illes Balears, IAC3-IEEC, E-07122 Palma de Mallorca, Spain
- ¹¹⁵ University of Rhode Island, 45 Upper College Road, Kingston, RI 02881, USA
- ¹¹⁶ The University of Texas Rio Grande Valley, Brownsville, TX 78520, USA
- ¹¹⁷ Bellevue College, Bellevue, WA 98007, USA
- ¹¹⁸ Institute for Plasma Research, Bhat, Gandhinagar 382428, India
- ¹¹⁹ The University of Sheffield, Sheffield S10 2TN, UK
- ¹²⁰ California State University, 5151 State University Drive, Los Angeles, CA 90032, USA
- ¹²¹ Dipartimento di Fisica, Università di Trento, I-38123 Povo, Trento, Italy
- ¹²² Montclair State University, Montclair, NJ 07043, USA
- ¹²³ National Astronomical Observatory of Japan, 2-21-1 Osawa, Mitaka, Tokyo 181-8588, Japan
- ¹²⁴ Canadian Institute for Theoretical Astrophysics, University of Toronto, Toronto, ON M5S 3H8, Canada
- ¹²⁵ Observatori Astronòmic, Universitat de València, E-46980 Paterna, València, Spain
- ¹²⁶ School of Mathematics, University of Edinburgh, Edinburgh EH9 3FD, UK
- ¹²⁷ University and Institute of Advanced Research, Koba Institutional Area, Gandhinagar Gujarat 382007, India
- ¹²⁸ Indian Institute of Technology, Bombay, India
- ¹²⁹ University of Szeged, Dóm tér 9, Szeged 6720, Hungary
- ¹³⁰ Tata Institute of Fundamental Research, Mumbai 400005, India
- ¹³¹ INAF, Osservatorio Astronomico di Capodimonte, I-80131 Napoli, Italy
- ¹³² University of Michigan, Ann Arbor, MI 48109, USA
- ¹³³ Abilene Christian University, Abilene, TX 79699, USA
- ¹³⁴ American University, Washington, DC 20016, USA
- ¹³⁵ University of Białystok, 15-424 Białystok, Poland
- ¹³⁶ University of Southampton, Southampton SO17 1BJ, UK
- ¹³⁷ University of Washington Bothell, 18115 Campus Way NE, Bothell, WA 98011, USA
- ¹³⁸ Institute of Applied Physics, Nizhny Novgorod, 603950, Russia
- ¹³⁹ Korea Astronomy and Space Science Institute, Daejeon 34055, Republic of Korea
- ¹⁴⁰ Inje University Gimhae, South Gyeongsang 50834, Republic of Korea
- ¹⁴¹ National Institute for Mathematical Sciences, Daejeon 34047, Republic of Korea
- ¹⁴² Ulsan National Institute of Science and Technology, 50 UNIST-gil, Eonyang-eup, Ulju-gun, Ulsan, Republic of Korea
- ¹⁴³ NCBJ, 05-400 Świerk-Otwock, Poland
- ¹⁴⁴ Institute of Mathematics, Polish Academy of Sciences, 00656 Warsaw, Poland
- ¹⁴⁵ Cornell University, Ithaca, NY 14850, USA
- ¹⁴⁶ Hillsdale College, Hillsdale, MI 49242, USA
- ¹⁴⁷ Hanyang University, Seoul 04763, Republic of Korea
- ¹⁴⁸ NASA Marshall Space Flight Center, Huntsville, AL 35811, USA
- ¹⁴⁹ Dipartimento di Fisica, Università degli Studi Roma Tre, I-00154 Roma, Italy
- ¹⁵⁰ INFN, Sezione di Roma Tre, I-00154 Roma, Italy
- ¹⁵¹ ESPCI, CNRS, F-75005 Paris, France
- ¹⁵² Southern University and A&M College, Baton Rouge, LA 70813, USA
- ¹⁵³ College of William and Mary, Williamsburg, VA 23187, USA
- ¹⁵⁴ Centre Scientifique de Monaco, 8 quai Antoine 1er, MC-98000, Monaco
- ¹⁵⁵ Indian Institute of Technology Madras, Chennai 600036, India
- ¹⁵⁶ INFN Sezione di Torino, Via P. Giuria 1, I-10125 Torino, Italy
- ¹⁵⁷ Institut des Hautes Etudes Scientifiques, F-91440 Bures-sur-Yvette, France
- ¹⁵⁸ IISER-Kolkata, Mohanpur, West Bengal 741252, India
- ¹⁵⁹ Whitman College, 345 Boyer Avenue, Walla Walla, WA 99362 USA
- ¹⁶⁰ Scuola Normale Superiore, Piazza dei Cavalieri 7, I-56126 Pisa, Italy
- ¹⁶¹ Université de Lyon, F-69361 Lyon, France
- ¹⁶² Hobart and William Smith Colleges, Geneva, NY 14456, USA
- ¹⁶³ Università degli Studi di Firenze, I-50121 Firenze, Italy
- ¹⁶⁴ OzGrav, Swinburne University of Technology, Hawthorn, VIC 3122, Australia
- ¹⁶⁵ Janusz Gil Institute of Astronomy, University of Zielona Góra, 65-265 Zielona Góra, Poland
- ¹⁶⁶ University of Washington, Seattle, WA 98195, USA
- ¹⁶⁷ SUPA, University of the West of Scotland, Paisley PA1 2BE, UK
- ¹⁶⁸ King's College London, University of London, London WC2R 2LS, UK
- ¹⁶⁹ Indian Institute of Technology, Gandhinagar Ahmedabad Gujarat 382424, India
- ¹⁷⁰ Indian Institute of Technology Hyderabad, Sangareddy, Khandi, Telangana 502285, India
- ¹⁷¹ International Institute of Physics, Universidade Federal do Rio Grande do Norte, Natal RN 59078-970, Brazil
- ¹⁷² Villanova University, 800 Lancaster Avenue, Villanova, PA 19085, USA
- ¹⁷³ Andrews University, Berrien Springs, MI 49104, USA
- ¹⁷⁴ Università di Siena, I-53100 Siena, Italy

¹⁷⁵ Trinity University, San Antonio, TX 78212, USA¹⁷⁶ Van Swinderen Institute for Particle Physics and Gravity, University of Groningen, Nijenborgh 4,
9747 AG Groningen, The Netherlands¹⁷⁷ Colorado State University, Fort Collins, CO 80523, USA

Received 2018 October 5; revised 2018 November 27; accepted 2018 December 7; published 2019 January 24

Abstract

We present a search for prompt gamma-ray counterparts to compact binary coalescence gravitational wave (GW) candidates from Advanced LIGO's first observing run (O1). As demonstrated by the multimessenger observations of GW170817/GRB 170817A, electromagnetic and GW observations provide complementary information about the astrophysical source, and in the case of weaker candidates, may strengthen the case for an astrophysical origin. Here we investigate low-significance GW candidates from the O1 compact binary coalescence searches using the *Fermi* Gamma-Ray Burst Monitor (GBM), leveraging its all sky and broad energy coverage. Candidates are ranked and compared to background to measure the significance. Those with false alarm rates (FARs) of less than 10^{-5} Hz (about one per day, yielding a total of 81 candidates) are used as the search sample for gamma-ray follow-up. No GW candidates were found to be coincident with gamma-ray transients independently identified by blind searches of the GBM data. In addition, GW candidate event times were followed up by a separate targeted search of GBM data. Among the resulting GBM events, the two with the lowest FARs were the gamma-ray transient GW150914-GBM presented in Connaughton et al. and a solar flare in chance coincidence with a GW candidate.

Key words: gamma-ray burst: general – gravitational waves

1. Introduction

The first observing run (O1) of the Advanced LIGO detectors (Aasi et al. 2015) marked the dawn of gravitational wave (GW) astronomy with the groundbreaking discovery of merging black holes (BHs; Abbott et al. 2016e, 2016g) and Abbott et al. (2016b). The second observing run (O2) continued unveiling the population of binary BHs (BBHs; Abbott et al. 2017b, 2017c, 2017d), saw the addition of the Virgo observatory to the detector network (Abbott et al. 2017d), and culminated in the spectacular multimessenger observations of a binary neutron star (BNS) merger, summarized in Abbott et al. (2017e, 2017f). Simultaneously observing the same astrophysical event in both gravitational and electromagnetic radiation will continue to uniquely enrich our understanding of sources. Because GWs negligibly interact with matter they are directly encoded with information about the central engines of the most violent, dynamic processes in the universe. Electromagnetic (EM) waves, on the other hand, are tightly coupled to matter thus providing information about the material and surrounding environment being affected by the central engine (Metzger & Berger 2012).

Several astrophysical transient phenomena are thought to produce GW and EM emission strong enough to be detected by current or proposed observatories, including soft gamma-ray repeaters, rapidly rotating core collapse supernovae, BNS mergers, and gamma-ray bursts. Here, we focus on short gamma-ray bursts (SGRBs), now directly confirmed to arise from the mergers of compact stellar remnants to which ground-based GW detectors are most sensitive (Abbott et al. 2017a). This paper is limited in scope to analysis of times during O1, and focuses on the follow-up searches of data from the *Fermi* Gamma-ray Burst Monitor (GBM) near in time to the GW

search candidates. Results for the search in GW data for known GRBs that occurred during O1 can be found in Abbott et al. (2017g).

Despite the consensus view that there would be no bright EM emission associated with stellar-mass BBH mergers, comprehensive observing campaigns with EM observatories were carried out. For example, 25 participating teams of observers received and responded to notifications of the GW150914 detection, with follow-up observations taken from the radio to gamma-ray bands (Abbott et al. 2016f). In the follow-up analysis of the time around the first BBH merger observation, GW150914, the *Fermi* GBM found a weak transient signal (Connaughton et al. 2016), GW150914-GBM, though no corresponding signal was observed in other gamma-ray instruments (Hurley et al. 2016; Savchenko et al. 2016; Tavani et al. 2016), nor was a similar signal found in relation to the other unambiguous GW detection in O1, GW151226 (Abbott et al. 2016e; Adriani et al. 2016; Racusin et al. 2017), though 85% of the LIGO localization for GW151226 was out of view by *Fermi*, occulted by the Earth (Racusin et al. 2017).

The case for a GW candidate too low in significance to be claimed as an unambiguous detection would be strengthened by an EM detection consistent with the putative GW event. To that end, this paper reports on the search of GBM data for potential EM counterparts to any GW binary merger candidates found in the O1 data set with a false alarm rate (FAR) below 10^{-5} Hz by the LIGO–Virgo analyses. Two GW candidates were identified in coincidence with gamma-ray signals exceeding the GBM background: a gamma-ray transient found in the follow-up of GW150914, previously reported in Connaughton et al. (2016), and a second GBM transient most likely due to a chance coincidence with a solar flare.

The paper is organized as follows. In Section 2, we describe the data analysis methods used to identify compact binary coalescence (CBC) triggers in GW data and to identify gamma-ray transients in the GBM data. Section 3 presents the search results. Section 4 summarizes the results and conclusions, and discusses the role for GBM and LIGO–Virgo joint analyses during future observing runs.

¹⁷⁸ Deceased, February 2018.¹⁷⁹ Deceased, November 2017.

2. Data Analysis Methods

2.1. Advanced LIGO

The LIGO observatories are two modified Michelson interferometers located in Livingston, Louisiana, and Hanford, Washington. Each arm of the interferometer is formed by two mirrors separated by 4 km. Passing GWs produce a strain, typically denoted as h , which changes the separation of the mirrors, inducing a relative phase difference in the light when it returns to the beam-splitter, which transmits an optical signal proportional to the incident strain. The large separation between the observatories reduces the false-alarm background due to coincident instrumental or environmental contamination, and differences in time and phase of arrival constrain the sky location of astrophysical sources. For a full description see Aasi et al. (2015).

The data are analyzed for continuous (Aasi et al. 2014b; Abbott et al. 2016h), stochastic (Abbott et al. 2016j), and transient astrophysical sources. Transient searches include “all sky” searches for new GW sources, and “targeted” searches for known astrophysical objects, e.g., GRBs (Abbott et al. 2017g) and supernovae (Abbott et al. 2016c). All sky sources can be divided into two broad classes: transients for which the GW signal is well modeled, enabling the use of template waveforms in matched filtering searches for BBHs (Abbott et al. 2016b), BNSs and NSBH systems (Abbott et al. 2016i), and cosmic strings (Aasi et al. 2014a); and “unmodeled” sources for which excess power searches are used (Abbott et al. 2016a).

This work focuses on follow-up searches in GBM data of results from the template-based all sky search for CBC events, i.e., transient signals from the final stages of binaries containing compact stellar remnants (BHs and/or NSs) as GW emission drives the objects to coalescence. Because the GWs from CBC sources are well modeled and computationally tractable (see, for example, Buonanno & Damour 1999; Blanchet 2006; Ajith et al. 2007), data analysis strategies for such sources rely on template waveforms.

The candidate sources for GBM follow-up were acquired from two independently developed CBC search pipelines, PyCBC (Dal Canton et al. 2014; Usman et al. 2016; Nitz et al. 2017) and GstLAL (Privitera et al. 2014; Messick et al. 2017). Here, we briefly summarize both searches. For a more detailed descriptions see Abbott et al. (2016d) and Abbott et al. (2016b). Both PyCBC and GstLAL use accurate models of the gravitational waveform from coalescing binaries to perform a phase-coherent matched filtering search. The mass and spin parameter space of plausible CBC signals is covered by a grid of $\mathcal{O}(10^5)$ points and a *template waveform* is computed at each point. The pipelines cover a total mass range between $2 M_{\odot}$ and $100 M_{\odot}$ with mass ratio from 1 to ~ 100 . The component spins are assumed to be parallel to the orbital angular momentum. Their dimensionless magnitudes can range from 0 to ~ 0.99 for components heavier than $2 M_{\odot}$ and from 0–0.05 for components lighter than $2 M_{\odot}$. Each template is correlated with the detectors’ strain data to calculate the signal-to-noise ratio (S/N). Data for which the same template produces a S/N above the pre-established detection threshold in each detector within 15 ms (slightly longer than the light travel time between detectors), are promoted to *coincident triggers* and ranked with a “network statistic,” which while different for PyCBC and GstLAL, is a function of the single-detector S/Ns and a measure of how consistent the data are with the template

waveform. Both pipelines estimate the background distribution of the network statistic in the absence of GWs, which is then used to map the network rank of each coincident trigger to the FAR of the search. In the remainder of this work, the FAR from the GW searches will be referred to by FAR_{GW} . Candidates with FAR_{GW} less than one per month exceeded the threshold for alerting EM observing partners participating in the O1 follow-up program (e.g., Abbott et al. 2016f). *Fermi* GBM has a unique data-sharing agreement with the LIGO Scientific and Virgo Collaborations, and has access to all CBC coincident triggers.

Because of their different assumptions and implementation details, PyCBC and GstLAL may produce different sets of triggers from the same data. Strong CBC signals are ranked by either pipeline to correspond to sufficiently low FAR_{GW} , although not numerically equal between pipelines. However, a weak signal can in principle be detected by only one pipeline. For this reason, here we combine the triggers produced by both pipelines into a superset of CBC candidates. For duplicate triggers found by both pipelines, we select the candidate with the lowest FAR_{GW} . The time range covered by the trigger set is from 2015 September 12 to 2016 January 19, with a total two-detector live-time of ~ 50 days. Approximately 10^4 triggers were recorded by PyCBC and GstLAL. In keeping with the spirit of an “eyes-wide-open” search for gamma-ray counterparts, no selection cuts were made to select for CBC candidates favoring systems theorized to produce potential electromagnetic counterparts (i.e., binaries containing at least one NS, and in the case of NSBHs, a sufficiently comparable mass ratio to tidally disrupt the NS).

The CBC searches were repeated when improvements to the calibration of the detectors or the configuration of the pipelines were available. The triggers employed in the joint analyses were obtained from the first analysis using the offline CBC pipelines, and an intermediate calibration of the data. Data produced with the final calibration were not available at the onset of this study. The candidate list used here was compared to that produced using the final calibration, and the only differences between the two were consistent with random noise fluctuations around the detection threshold of the CBC searches.

2.2. Fermi GBM

The *Fermi* GBM is an all-sky instrument onboard NASA’s *Fermi* Gamma-ray Space Telescope. The GBM has an instantaneous field of view that subtends 70% of the celestial sphere (with the remaining 30% occulted by the Earth), with an 85% live-time, and energy coverage from 8 keV to 40 MeV. These capabilities make GBM an ideal partner in the searches for joint detections with ground-based GW observatories. The omnidirectional, broad energy coverage is accomplished through the use of 12 sodium iodide (NaI) detectors and two bismuth germanate (BGO) detectors.

The responses for the NaI detectors are strongly dependent on the incident angle to the source, while the responses for the BGO detectors are not. Additionally, responses from all detectors are dependent on the source spectrum, since the blockage or attenuation of photons by the spacecraft and scattering off spacecraft components are energy dependent. These properties of the response will cause a signal to appear with a different strength in each detector, and the relative observed strength between all detectors allows the localization

of signals with an accuracy on the order of a few to tens of degrees (Connaughton et al. 2015). In practice, the expected photon rates at each detector are calculated over a grid of possible source spectrum templates and sky locations, and the observed relative rates are then compared to this expectation.

There are currently three distinct searches used on GBM data in the joint analysis of GW sources: the onboard *triggering* algorithm for automatic detection of strong GRBs (Meegan et al. 2009; von Kienlin et al. 2014; Bhat et al. 2016); the ground-based *untargeted* search for weak SGRBs; and the *targeted* search used for follow-up GW candidates (Blackburn et al. 2015). The onboard triggering and ground-based untargeted GBM searches are the means by which SGRBs are identified in the GBM data without any input about when or where a possible GW source may have occurred. The targeted search of GBM data uses as input the arrival time of a GW candidate and uses the angular and energy dependencies of the detector response to find spectrally and spatially coherent weak signals.

2.2.1. Blind, Untargeted GRB Searches

The GBM flight software will trigger on board when count rates in the time-binned data of two or more NaI detectors exceed the background count rates, determined by averages of ~ 15 s of the previous data, by pre-specified thresholds (typically 4.5σ). The onboard trigger is activated by approximately 40 SGRBs/year. For a full description of GBM and the onboard triggering algorithm see (Meegan et al. 2009; von Kienlin et al. 2014; Bhat et al. 2016).

The untargeted, ground-based analysis searches primarily for SGRBs in continuous time-tagged event data. While a full description of the untargeted search will be in a forthcoming article we present a brief description here. The primary science goal of the search is to rapidly identify SGRBs missed by the triggering algorithm in order to maximize the potential for multimessenger observations, either through GW follow-up searches or to identify counterparts to astrophysical neutrinos. The analysis searches for signals with durations ranging from 64 ms to 32 s. Candidates are identified when two NaI detectors have an excess number of counts, with one exceeding 2.5 standard deviations (σ) relative to the background, and at least one other exceeding 1.25σ . Correcting for the number of time bins in a day, the Poisson probability of the excess in the two detectors must be less than 10^{-6} . The untargeted search is currently finding approximately 80 SGRB candidates per year in addition to those found by the onboard triggering algorithm.¹⁸⁰

2.2.2. Follow-up Targeted GRB Search

The targeted search was developed to examine GBM data for gamma-ray transients in coincidence with GW candidates from LIGO’s sixth science run (S6) and the concurrent second and third science runs (VSR2 and VSR3, respectively) of the Virgo 3 km interferometer in Cascina, Italy (Accadia et al. 2012). A description of how this method was applied to the S6+VSR2/3 data is presented in Blackburn et al. (2015).

The targeted search identifies candidate gamma-ray transients over a 60 s window centered on the GW trigger time. The 60 s time window is a conservative choice to not exclude

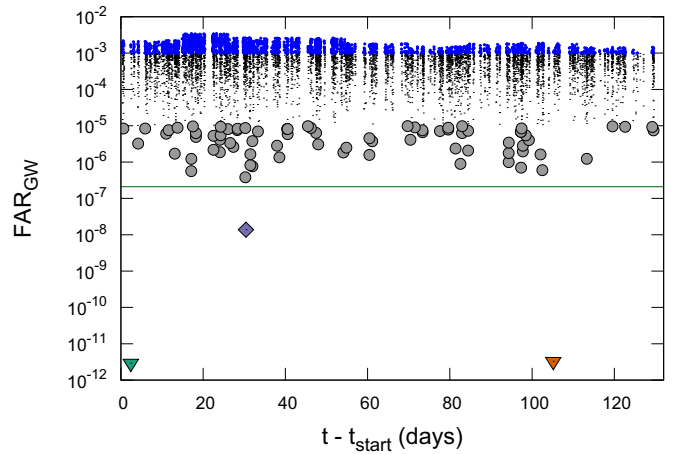


Figure 1. Time series of CBC triggers relative to the start-time of the joint analysis (September 12, windows 2015). The horizontal line denotes the inverse live-time for the search sample (~ 50 days). The joint GBM/LIGO analyses used the blue points as the background sample, with $\text{FAR}_{\text{GW}} > 10^{-3}$ Hz. The gray circles correspond to the search sample, with $\text{FAR}_{\text{GW}} < 10^{-5}$ Hz, or approximately fewer than one per day. The green and orange downward-pointing triangles correspond to the upper limits on FAR_{GW} for GW150914 and GW151226, respectively. The purple diamond corresponds to LVT151012. These colors and marker styles are preserved throughout the article.

precursor EM emission from the merger, or a delay between the compact objects’ coalescence and launching of the relativistic jet. Operating during O1, the targeted search utilized the daily continuous time (CTIME) data, with a nominal time resolution of 256 ms and 8 energy channels. The search was performed on binned data with bin-widths ranging from 256 ms to 8.192 s.

The targeted search uses three template spectra to coherently forward model the detector response. The templates are Band spectra (Band et al. 1993) comprised of two power-law components with spectral indices α and β smoothly joined at the energy, E_{peak} . The definition of E_{peak} , and therefore the spectral model, are modified from the original definition in Band et al. (1993) and are explicitly shown in Connaughton et al. (2015). The templates are referred to as “soft,” “normal,” and “hard” spectra with Band function parameters α , β , $E_{\text{peak}} = (-1.9, -3.7, 70 \text{ keV})$, $(-1, -2.3, 230 \text{ keV})$, and $(0, -1.5, 1 \text{ MeV})$, respectively. Each of the templates are utilized independently during the search, and then the most significant spectrum is identified for each time bin of the search.

The detection statistic Λ for the targeted search is derived from a log likelihood ratio formalism that measures the GBM signal strength relative to a polynomial fit to the background count rate. A detailed discussion of the search’s methodology can be found in Blackburn et al. (2015).

3. Search Results

3.1. Advanced LIGO Sample

Figure 1 shows times relative to the start of the search sample (2015 September 12) for the combined CBC triggers produced by the `GstLAL` and `PyCBC` pipelines. Intervals with no triggers correspond to times when one or both detectors were unable to produce science data, or when the data were vetoed due to well-understood instrumental or environmental disturbances. With the exception of the two high-confidence detections GW150914 (green triangle) (Abbott et al. 2016g)

¹⁸⁰ https://gcn.gsfc.nasa.gov/admin/fermi_gbm_subthreshold_announce.txt

and GW151226 (orange triangle) (Abbott et al. 2016e), and the low-significance candidate LVT151012 (purple diamond) (Abbott et al. 2016b), no CBC triggers were more significant than the inverse live-time of the search $\sim 2 \times 10^{-7}$ Hz (black horizontal line). For the targeted GBM search, the 81 subthreshold candidates with $\text{FAR}_{\text{GW}} < 10^{-5}$ Hz ($\lesssim 1$ day $^{-1}$) marked by gray circles were used as the search sample, while the 2935 blue dots ($\text{FAR}_{\text{GW}} > 10^{-3}$ Hz) served as the background sample. The candidates between the background and search samples (black dots) were discarded for two reasons. First, to avoid the scenario where the background and search samples were sufficiently close in significance that the determination of which sample a candidate belonged in was up to random chance. Second, due to the long tails in the GBM search statistics, the threshold used for the background sample provided sufficient triggers to measure the significance of anything in the search sample, making the inclusion of additional background triggers unnecessary.

3.2. Triggering and Untargeted Search

The simplest step in the joint analysis is to compare the list of times of known gamma-ray transients to the list of times of CBC candidates and search for a match. This comparison is complementary to the dedicated follow-up of known GRBs in GW data of GRBs, as reported in Abbott et al. (2017g) in two ways: first, here we do not impose a maximum time offset between the GW and gamma-ray candidates, and second, this study includes subthreshold GBM candidates from the untargeted search, which in O1, were not incorporated in the LIGO–Virgo GRB follow-up searches.

For the joint analysis, events found in the GBM triggering and untargeted searches during O1 are combined and correlated with the combined list of CBC candidates, searching for coincident events in the two observatories. The GBM trigger list includes 115 GRBs, about half of which are SGRBs. The search statistic is the shortest absolute time offset between a GRB and the search sample of CBC triggers, allowing for the possibility that the EM signal can precede or follow the compact binary merger event.

Using CBC candidates with $\text{FAR}_{\text{GW}} > 10^{-3}$ Hz as a background sample (blue dots in Figure 1) and $\text{FAR}_{\text{GW}} < 10^{-5}$ as the search sample, we find the 90th percentile of the absolute offset time from the closest GRB in our sample to be $\sim 10^4$ s. Approximately 10% of the search sample is closer in time to a GRB, as expected for a null result based on the background sample. The agreement between cumulative distribution functions of the absolute time offset $|\Delta T|$ for the background sample (blue dotted line) and the search sample (gray solid line) is shown in Figure 2. The shortest interval between the event times of a triggered GRB and a CBC candidate was $|\Delta T| = 426.26$ s.

3.3. Targeted Search

The targeted search follow-up of PyCBC and GstLAL CBC coincident triggers used the same selection criteria as described earlier, with an additional down-selection of triggers, which appeared in both CBC pipelines within 1 s of each other, in which case the trigger with the highest FAR_{GW} was removed from the sample. By this procedure, there were 17 times that a trigger was found by both pipelines: nine triggers with no offset ($|\Delta T| < 0.01$ s), seven triggers with offset of $|\Delta T| \sim 0.01$ s,

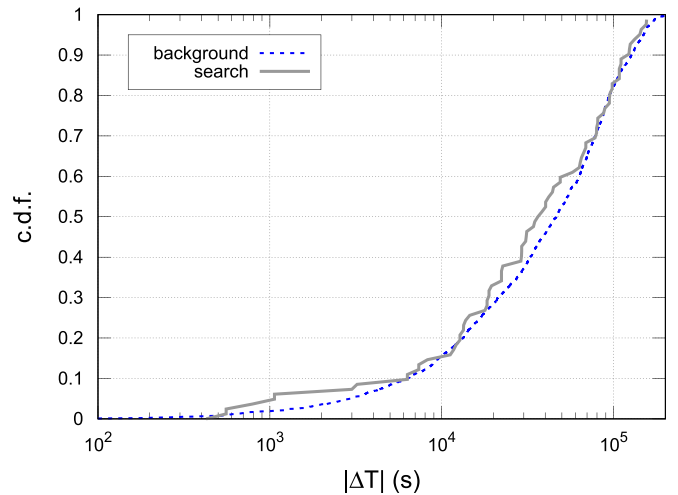


Figure 2. Cumulative distribution function of minimum absolute offset time between a GRB found by the triggered or untargeted GBM searches and a CBC candidate. The search sample (gray solid line) is consistent with the background distribution (blue dotted line), indicating that there are no significant coincidences between independently identified GBM and CBC triggers during O1.

and one occurrence with an offset of $|\Delta T| \sim 0.02$ s. Of the remaining times of interest, 10% occur when *Fermi* was not taking data due to transit of the South Atlantic Anomaly (SAA), consistent with expectations. There were no cases where *Fermi* entered or exited the SAA during the 60 s search interval. For the remaining GW triggers with GBM data, GBM observed between 52% and 92% of the GW sky map probability, with an average observing fraction of 69%. Figure 3 shows the cumulative event rate of the GBM background and search samples as a function of the detection statistic Λ . The distribution of the search samples is largely consistent with that of the background.

The GBM FAR, FAR_{GBM} , for coincidences in the targeted follow-up of CBC candidates with $\text{FAR}_{\text{GW}} < 10^{-5}$ Hz can be mapped to a false alarm probability (FAP) p -value. Here, the p -value is similar to the quantity defined as the FAP in Connaughton et al. (2016), which used an analytic approximation to estimate the significance of a candidate.

However, the significance calculation used in this work differs from that in Connaughton et al. (2016). For a given candidate found in the GBM follow-up search, the FAP is intended to report the probability of detecting a false associated signal (either statistical fluctuation or real unassociated signal) with a ranking that is at least as significant as the candidate.

As in Connaughton et al. (2016), search candidates are first ranked by $R = 1/(\text{FAR}_{\text{GBM}}|\Delta T|)$, where FAR_{GBM} is the cumulative event rate of the background distribution at the candidate’s value for the search statistic (see Figure 3), and $|\Delta T|$ is the absolute value of the time offset between the closest GW trigger time and the GBM candidate. We impose a minimum ΔT_{min} equal to the bin-width of the GBM data, which is 256 ms.

For this analysis we empirically measure the FAP by using background noise events from the GW searches to seed GBM follow-up. Background events are ranked using the same statistic R . The FAP of a candidate event is the p -value of the background distribution with that candidate’s ranking statistic, R .

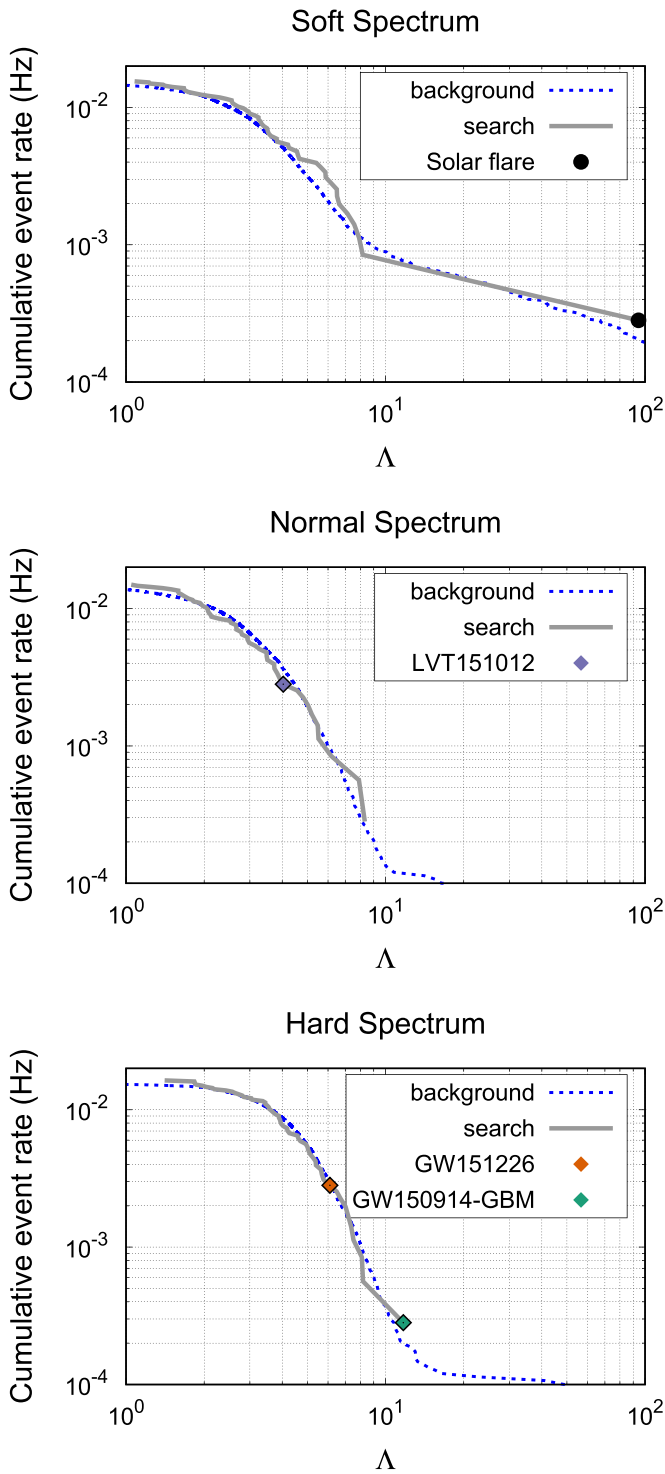


Figure 3. Cumulative event rates of the background (blue dotted lines) and search (gray solid lines) samples for the GBM targeted follow-up of CBC triggers as a function of the detection statistic Λ . The panels in the figure from top to bottom correspond to results from the soft, normal, and hard template spectra. The distribution of the search samples is largely consistent with that of the background. The two most significant events from the search distribution are the GBM transient identified in the follow-up to GW150914 (green diamond) and a soft, long-duration, transient found 26 s after a low-significance GW trigger. The long, soft transient is likely due to solar activity, and in a chance coincidence with a GW trigger.

Figure 4 shows the cumulative distribution of p -values for all of the CBC triggers follow-up candidates. GW150914-GBM had the lowest p -value of any follow-up event, due to the fact

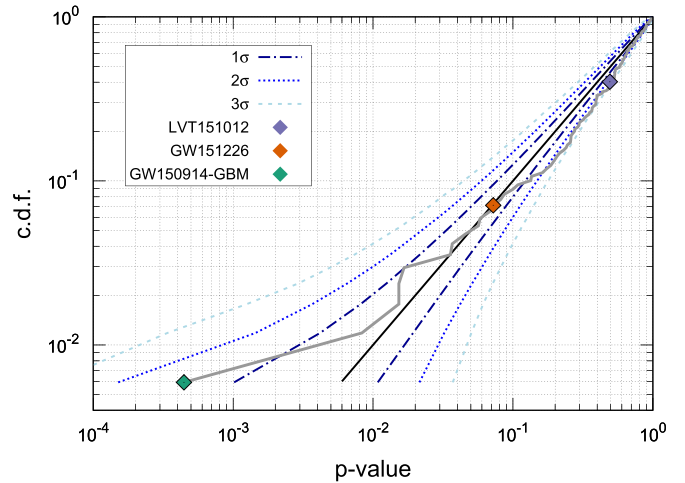


Figure 4. Cumulative distribution function of empirically determined p -values for the targeted search. The black solid line corresponds to the null hypothesis that the search sample is consistent with background. The blue dashed lines envelop the 1- σ , 2- σ , and 3- σ confidence intervals. The highest ranking (lowest p -value) event is GW150914-GBM (green diamond), which for this search, has a significance of $\gtrsim 1.5\sigma$.

that it had both the lowest FAR_{GBM} and had the shortest time offset to its GW trigger time. The p -value for GW150914-GBM is an upper bound, because although there were more significant events in the background sample as determined by detection statistic Λ , the short time offset from the GW trigger caused it to have a higher ranking statistic, R , than any of the events in the background distribution. The blue dashed lines envelop the expected 1- σ (dark blue) 2- σ (blue), and 3- σ (light blue) confidence intervals, assuming that the search distribution is statistically identical to the background distributions based on the number of events analyzed. From this it is clear that GW150914-GBM is a $\gtrsim 1.5\sigma$ event. This is a lower significance than reported in Connaughton et al. (2016) owing to the large number of CBC events in the search sample, due to the low threshold chosen for trigger selection. This was intentional, as the point of this study was to search for subthreshold joint detections, and we treat all CBC candidates in the search sample as equally worthwhile of follow-up.

Also note that the second lowest FAR ($\text{FAR}_{\text{GBM}} = 2.6 \times 10^{-4}$ Hz) of the search occurred in the analysis of the GBM transient detected at 2015 September 29 12:15:43.6 UTC. The event was at the edge of the search window, 26 s before the GW trigger time that prompted the GBM analysis, resulting in p -value ~ 1 . The event was found using the soft template and the longest (8.192 s) timescale of the search. A search for other possibly associated astrophysical transients at that time revealed that the GBM event occurred during the exponential decay tail of an M-class solar flare (e.g., GBM triggers 150929346 and 150929553). The GBM localization for this candidate is consistent with the Sun and inconsistent with the LIGO sky map, thus we conclude this GBM event is due to solar activity.

4. Conclusions and Discussion

The GBM follow-up analyses searched for gamma-ray transients associated with a list of CBC candidates during O1. These CBC candidates were well below the standards for the GW trigger alone to be considered likely due to a compact

merger, but significant enough that if a gamma-ray transient was found by GBM in coincidence, it would support an astrophysical origin of the GW transient.

There were no coincidences between GBM transients found by the triggered or untargeted searches and the LIGO CBC candidates. For the targeted follow-up of GW candidates, GW150914-GBM is the most significant event of the search. The analysis presented here was not designed to revisit the significance of the GW150914-GBM association; additional observations of BBH mergers with GBM will be needed to establish or rule out the astrophysical nature of GW150914-GBM. No other significant transients were found in the GBM targeted search, ruling out the possibility of a low-significance GW event being identified by its association with a gamma-ray transient during O1.

The significance of GW150914-GBM reported by the search described in this paper ($\gtrsim 1.5\sigma$) is conservative in part because of the choice to not include in the candidate ranking the significance of the GW triggers. By not using the GW significance in our assessment of the validity of a GBM counterpart, the targeted search is hampered by implicitly placing marginal GW events on equal footing with more plausible ones. Joint GW/EM events may prove to be rare, and the search strategy as adopted is to cast a wide, model-independent, net when looking for possible subthreshold coincidences in both observatories. Deriving a joint significance that includes information about the likelihood of the GW candidate being astrophysical is subtle; having a high-significance GW event does not necessarily imply a high likelihood for an associated gamma-ray transient. Incorporating the significance of the GW candidate into the GBM follow-up analysis is an area of investigation for future joint observing campaigns (Ashton et al. 2017).

For the targeted search, the long tails in the background distribution out to high values of the ranking statistic limited the sensitivity of the search in O1. Further analysis has revealed that many ($>20\%$) of the high likelihood events in the background can be attributed to large background fluctuations due to high particle activity associated with *Fermi*'s proximity to the SAA. For analyses of later observing runs, the background fitting procedure and the vetoing of data from entry and exit of the SAA have been improved (Goldstein et al. 2016).

The multimessenger observations of the BNS merger associated with a short GRB, and the resulting kilonova and GRB afterglow observations, demonstrated a best-case scenario of a bright, nearby transient, which was identified unambiguously gravitationally and electromagnetically. However, the event had the closest recorded redshift for any GRB despite its relatively low brightness (Goldstein et al. 2017), while the BNS system was well within the detection horizon for the LIGO–Virgo network (Abbott et al. 2017e). It is therefore not difficult to imagine scenarios where subthreshold searches would have been critical for identifying the association. Joint analyses that can elevate the significance of candidate events are needed to best exploit the rich data sets from GW and gamma-ray survey instruments. The searches reported here, while not producing any unambiguous counterparts, will serve as a foundation for future joint analysis.

The USRA co-authors gratefully acknowledge NASA funding through contract NNM13AA43C. The UAH co-authors gratefully

acknowledge NASA funding from co-operative agreement NNM11AA01A. E.B. and T.D.C. are supported by an appointment to the NASA Postdoctoral Program at the Goddard Space Flight Center, administered by Universities Space Research Association under contract with NASA. D.K., C.A.W.H., C.M. H., and T.L. gratefully acknowledge NASA funding through the *Fermi* GBM project. Support for the German contribution to GBM was provided by the Bundesministerium für Bildung und Forschung (BMBF) via the Deutsches Zentrum für Luft und Raumfahrt (DLR) under contract number 50 QV 0301. A.v.K. was supported by the Bundesministeriums für Wirtschaft und Technologie (BMWi) through DLR grant 50 OG 1101. N.C. and J.B. acknowledge support from NSF under grant PHY-1505373. S.M.B. acknowledges support from Science Foundation Ireland under grant 12/IP/1288.

The authors gratefully acknowledge the support of the United States National Science Foundation (NSF) for the construction and operation of the LIGO Laboratory and Advanced LIGO as well as the Science and Technology Facilities Council (STFC) of the United Kingdom, the Max-Planck-Society (MPS), and the State of Niedersachsen/Germany for support of the construction of Advanced LIGO and construction and operation of the GEO600 detector. Additional support for Advanced LIGO was provided by the Australian Research Council. The authors gratefully acknowledge the Italian Istituto Nazionale di Fisica Nucleare (INFN), the French Centre National de la Recherche Scientifique (CNRS) and the Foundation for Fundamental Research on Matter supported by the Netherlands Organisation for Scientific Research, for the construction and operation of the Virgo detector and the creation and support of the EGO consortium. The authors also gratefully acknowledge research support from these agencies as well as by the Council of Scientific and Industrial Research of India, the Department of Science and Technology, India, the Science & Engineering Research Board (SERB), India, the Ministry of Human Resource Development, India, the Spanish Agencia Estatal de Investigación, the Vicepresidència i Conselleria d'Innovació Recerca i Turisme and the Conselleria d'Educació i Universitat del Govern de les Illes Balears, the Conselleria d'Educació Investigació Cultural i Esport de la Generalitat Valenciana, the National Science Centre of Poland, the Swiss National Science Foundation (SNSF), the Russian Foundation for Basic Research, the Russian Science Foundation, the European Commission, the European Regional Development Funds (ERDF), the Royal Society, the Scottish Funding Council, the Scottish Universities Physics Alliance, the Hungarian Scientific Research Fund (OTKA), the Lyon Institute of Origins (LIO), the National Research, Development and Innovation Office Hungary (NKFI), the National Research Foundation of Korea, Industry Canada and the Province of Ontario through the Ministry of Economic Development and Innovation, the Natural Science and Engineering Research Council Canada, the Canadian Institute for Advanced Research, the Brazilian Ministry of Science, Technology, Innovations, and Communications, the International Center for Theoretical Physics South American Institute for Fundamental Research (ICTP-SAIFR), the Research Grants Council of Hong Kong, the National Natural Science Foundation of China (NSFC), the Leverhulme Trust, the Research Corporation, the Ministry of Science and Technology (MOST), Taiwan and the Kavli Foundation. The authors gratefully acknowledge the support of the NSF, STFC,

MPS, INFN, CNRS, and the State of Niedersachsen/Germany for provision of computational resources.

ORCID iDs

L. Blackburn <https://orcid.org/0000-0002-9030-642X>
 P. Veres <https://orcid.org/0000-0002-2149-9846>
 E. Bissaldi <https://orcid.org/0000-0001-9935-8106>
 A. von Kienlin <https://orcid.org/0000-0002-0221-5916>
 F. Aubin <https://orcid.org/0000-0002-8241-4156>
 C. Aulbert <https://orcid.org/0000-0002-1481-8319>
 I. Bartos <https://orcid.org/0000-0001-5607-3637>
 B. Bécsy <https://orcid.org/0000-0003-0909-5563>
 C. Beer <https://orcid.org/0000-0003-3991-067X>
 M. Bejger <https://orcid.org/0000-0002-4991-8213>
 S. Bernuzzi <https://orcid.org/0000-0002-2334-0935>
 R. Ciolfi <https://orcid.org/0000-0003-3140-8933>
 N. Cornish <https://orcid.org/0000-0002-7435-0869>
 A. Corsi <https://orcid.org/0000-0001-8104-3536>
 M. W. Coughlin <https://orcid.org/0000-0002-8262-2924>
 Z. Doctor <https://orcid.org/0000-0002-2077-4914>
 H.-B. Eggenstein <https://orcid.org/0000-0001-5296-7035>
 S. Fairhurst <https://orcid.org/0000-0001-8480-1961>
 B. Farr <https://orcid.org/0000-0002-2916-9200>
 W. M. Farr <https://orcid.org/0000-0003-1540-8562>
 M. Fishbach <https://orcid.org/0000-0002-1980-5293>
 B. Giacomazzo <https://orcid.org/0000-0002-6947-4023>
 A. Grado <https://orcid.org/0000-0002-0501-8256>
 C.-J. Haster <https://orcid.org/0000-0001-8040-9807>
 D. E. Holz <https://orcid.org/0000-0002-0175-5064>
 V. Kalogera <https://orcid.org/0000-0001-9236-5469>
 D. Keitel <https://orcid.org/0000-0002-2824-626X>
 P. Koch <https://orcid.org/0000-0003-2777-5861>
 B. Krishnan <https://orcid.org/0000-0003-3015-234X>
 J. Lange <https://orcid.org/0000-0002-2450-1366>
 P. D. Lasky <https://orcid.org/0000-0003-3763-1386>
 C. O. Lousto <https://orcid.org/0000-0002-6400-9640>
 A. Markowitz <https://orcid.org/0000-0002-2173-0673>
 K. Mogushi <https://orcid.org/0000-0003-3746-2586>
 M. Obergaulinger <https://orcid.org/0000-0001-5664-1382>
 R. O’Shaughnessy <https://orcid.org/0000-0001-5832-8517>
 C. Pankow <https://orcid.org/0000-0002-1128-3662>
 F. Pannarale <https://orcid.org/0000-0002-7537-3210>
 V. Piero <https://orcid.org/0000-0002-6020-5521>
 M. Pitkin <https://orcid.org/0000-0003-4548-526X>
 P. Raffai <https://orcid.org/0000-0001-7576-0141>
 Javed Rana <https://orcid.org/0000-0001-5605-1809>
 F. Ricci <https://orcid.org/0000-0001-5742-5980>

N. Sarin <https://orcid.org/0000-0003-2700-1030>
 C. Talbot <https://orcid.org/0000-0003-2053-5582>
 K. Ueno <https://orcid.org/0000-0003-0424-3045>
 Hang Yu <https://orcid.org/0000-0002-6011-6190>
 M. Zevin <https://orcid.org/0000-0002-0147-0835>

References

- Aasi, J., Abadie, J., Abbott, B. P., et al. 2014a, *PhRvL*, 112, 131101
 Aasi, J., Abadie, J., Abbott, B. P., et al. 2014b, *ApJ*, 785, 119
 Aasi, J., Abadie, J., Abbott, B. P., et al. 2015, *CQGRa*, 32, 074001
 Abbott, B. P., Abbott, R., Abbott, T. D., et al. 2016a, *PhRvD*, 95, 042003
 Abbott, B. P., Abbott, R., Abbott, T. D., et al. 2016b, *PhRvX*, 6, 041015
 Abbott, B. P., Abbott, R., Abbott, T. D., et al. 2016c, *PhRvD*, 94, 102001
 Abbott, B. P., Abbott, R., Abbott, T. D., et al. 2016d, *PhRvD*, 93, 122003
 Abbott, B. P., Abbott, R., Abbott, T. D., et al. 2016e, *PhRvL*, 116, 241103
 Abbott, B. P., Abbott, R., Abbott, T. D., et al. 2016f, *PhRvL*, 119, 141101
 Abbott, B. P., Abbott, R., Abbott, T. D., et al. 2016g, *PhRvL*, 116, 061102
 Abbott, B. P., Abbott, R., Abbott, T. D., et al. 2016h, *PhRvD*, 94, 102002
 Abbott, B. P., Abbott, R., Abbott, T. D., et al. 2016i, *ApJL*, 832, L121
 Abbott, B. P., Abbott, R., Abbott, T. D., et al. 2016j, *PhRvL*, 118, 121101
 Abbott, B. P., Abbott, R., Abbott, T. D., et al. 2017a, *ApJL*, 848, L13
 Abbott, B. P., Abbott, R., Abbott, T. D., et al. 2017b, *PhRvL*, 118, 221101
 Abbott, B. P., Abbott, R., Abbott, T. D., et al. 2017c, *ApJL*, 851, L35
 Abbott, B. P., Abbott, R., Abbott, T. D., et al. 2017d, *PhRvL*, 119, 141101
 Abbott, B. P., Abbott, R., Abbott, T. D., et al. 2017e, *PhRvL*, 119, 161101
 Abbott, B. P., Abbott, R., Abbott, T. D., et al. 2017f, *ApJL*, 848, L12
 Abbott, B. P., Abbott, R., Abbott, T. D., et al. 2017g, *ApJ*, 841, 89
 Accadia, T., Acernese, F., Alshourbagy, M., et al. 2012, *JInst*, 7, P03012
 Adriani, O., Akaike, Y., Asano, K., et al. 2016, *ApJL*, 829, L20
 Ajith, P., Babak, S., Chen, Y., et al. 2007, *CQGRa*, 24, S689
 Ashton, G., Burns, E., Dal Canton, T., et al. 2017, *ApJ*, 860, 6
 Band, D., Matteson, J., Ford, L., et al. 1993, *ApJ*, 413, 281
 Bhat, P. N., Meegan, C. A., von Kienlin, A., et al. 2016, *ApJS*, 223, 28
 Bissaldi, E., von Kienlin, A., Lichti, G., et al. 2009, *ExA*, 24, 47
 Blackburn, L., Briggs, M. S., Camp, J., et al. 2015, *ApJS*, 217, 8
 Blanchet, L. 2006, *LRR*, 9, 4
 Buonanno, A., & Damour, T. 1999, *PhRvD*, 59, 084006
 Connaughton, V., Briggs, M. S., Goldstein, A., et al. 2015, *ApJS*, 216, 32
 Connaughton, V., Burns, E., Goldstein, A., et al. 2016, *ApJL*, 826, L6
 Dal Canton, T., Nitz, A. H., Lundgren, A. P., et al. 2014, *PhRvD*, 90, 082004
 Goldstein, A., Burns, E., Hamburg, R., et al. 2016, arXiv:1612.02395
 Goldstein, A., Veres, P., Burns, E., et al. 2017, *ApJL*, 848, L14
 Hurley, K., Svinikin, D. S., Aptekar, R. L., et al. 2016, *ApJL*, 829, L12
 Meegan, C., Lichti, G., Bhat, P. N., et al. 2009, *ApJ*, 702, 791
 Messick, C., Blackburn, K., Brady, P., et al. 2017, *PhRvD*, 95, 042001
 Metzger, B. D., & Berger, E. 2012, *ApJ*, 746, 48
 Nitz, A., Harry, I., Biwer, C. M., et al. 2017, ligo-cbc/pycbc: O2 Production Release 4, Zenodo, doi:10.5281/zenodo.249519
 Privitera, S., Mohapatra, S. R. P., Ajith, P., et al. 2014, *PhRvD*, 89, 024003
 Racusin, J. L., Burns, E., Goldstein, A., et al. 2017, *ApJ*, 835, 82
 Savchenko, V., Ferrigno, C., Mereghetti, S., et al. 2016, *ApJL*, 820, L36
 Tavani, M., Pittori, C., Verrecchia, F., et al. 2016, *ApJL*, 825, L4
 Usman, S. A., Nitz, A. H., Harry, I. W., et al. 2016, *CQGRa*, 33, 215004
 von Kienlin, A., Meegan, C. A., Paciasas, W. S., et al. 2014, *ApJS*, 211, 13